High temperature and low threshold interband cascade lasers at wavelengths longer than 6 μm

S.M. Shazzad Rassel, Lu Li, Yiyun Li, Rui Q. Yang*,

School of Electrical and Computer Engineering, University of Oklahoma, Norman, OK 73019, USA

James A. Gupta, X. Wu and Geof C. Aers

National Research Council of Canada, Ottawa, ON K1A 0R6 Canada

Abstract

InAs-based interband cascade (IC) lasers with improved optical confinement have achieved high-temperature operation with a threshold current density as low as 333 A/cm^2 at 300 K for emission at 6003 nm. The threshold current density is the lowest ever reported among semiconductor mid-infrared lasers at similar wavelengths. These InAs-based IC devices lased in pulsed mode at temperatures up to 357 K near 6.28 μm. A narrow-ridge device was able to operate in continuous-wave mode at temperatures up to 293 K at 6.01 μm.

Keywords: Interband cascade laser, type-II quantum well, mid-infrared, InAs.

* E-mail: Rui.Q.Yang@ou.edu

Interband cascade (IC) lasers were first proposed at a conference in 1994 [1], the same year when quantum cascade (QC) lasers based on intersubband transition were initially demonstrated [2]. From a historical perspective, the emergence of IC lasers evolved from the early pursuit of intersubband lasing and research on interband tunneling in type-II quantum well systems [3-7], which had been mentioned on several occasions [8-10]. Both IC and QC lasers share the characteristic benefit of cascade structures for reusing every injected electron to generate multiple photons with high quantum efficiencies and uniform carrier injection over every active stage. In principle, IC lasers should have the advantage that interband transitions have orders of magnitude longer carrier lifetime compared to that in QC lasers, where fast phonon scattering is inherent to intersubband transitions. However, despite the favorable results projected by theoretical calculations and arguments [11-12] and the fact that they appeared at about the same time, the amount of effort expanded in the development of IC lasers has been very limited as compared with QC lasers. Consequently, many aspects of IC lasers have been unexplored or remained in the early phase. This is partially attributed to the less mature Sb-based III-V material system and related device fabrication technology, as well as limited resources for the growth of Sb-based materials compared to more mature InP- and GaAs-based material systems and the widely available resources for them.

In the last decade, remarkable progress in developing IC lasers on GaSb substrates has been achieved mainly in the 3-4 μm wavelength region [13-19]. Low threshold current density (*e.g.* ~100 A/cm^2 at 3.6 μm) and low power consumption (<0.1 W) at room temperature [19] have led to growing applications in chemical sensing, including the detection of CH_4 on Mars [20]. By using type-I quantum well (QW) active regions, IC

lasers have extended emission wavelengths down to 2 μm with enhanced device performance [21]. On the longer wavelength side, by employing a plasmon waveguide approach on InAs substrates, which was initially used in QC lasers [22-23], IC lasers have been demonstrated at wavelengths beyond 6 μm and up to 11 μm [24-29]. Recently, efforts have been expanded to improving GaSb-based IC lasers at wavelengths approaching and beyond 6 μm [30-31]. At wavelengths near or beyond 6 μm, these reported IC lasers were operated at temperatures below 350 K in pulsed mode and their threshold current densities at room temperature were close to or higher than 500 A/cm^2 (*e.g.* 660 A/cm^2 at 6 μm [30]), so they could not lase in continuous wave (cw) mode at room temperature. In this paper, we report InAs-based IC lasers that are able to lase in pulsed mode at high temperatures (>350 K) with emission wavelengths beyond 6 μm and with significantly reduced threshold current density at room temperature (<400 A/cm^2). For the first time, cw operation of IC lasers is demonstrated at room temperature near 6.01 μm.

The IC laser structure was designed based on an improved waveguide configuration [32] with two 0.65-μm-thick undoped InAs separate confinement layers (SCLs), two 1.3-μm-thick InAs/AlSb/AlAs superlattice (SL) intermediate cladding layers, and highly-doped n^+-InAs (1.1×10^{19} cm^{-3}) outer cladding layers, which has been proven to be effective to enhance optical confinement and reduce the optical loss for InAs-based IC lasers near 4.6 μm compared to the early design [32]. In comparison with the GaSb-based IC lasers [19, 30-31] where GaSb is used for SCLs, the optical confinement factor for an InAs-based IC laser would be reduced if the same number of cascade stages is used because the refractive index of InAs is substantially smaller than that of GaSb. Hence, more cascade stages are desirable

for InAs-based IC lasers to achieve a comparable optical confinement factor. Nevertheless, the thermal dissipation can be improved and the growth of InAs-based IC lasers is easier because of significantly reduced thickness of SL cladding layer and without using mixed group-V InAsSb layers. Also, the carrier transport can be more efficient and smooth in InAs-based IC lasers without using an *n*-type GaSb layer (that has a significant higher conduction band-edge in constrast to InAs), possibly resulting in an improved voltage efficiency. In this work, the InAs-based IC laser structure comprises 15 cascade stages and was grown on an *n*-type InAs substrate in a V90 MBE system. The calculated band-edge diagram (based on a two-band model [7,33]) with a detailed layer sequence for one cascade stage is shown in Fig. 1. The central 2 InAs QWs in the electron injector of each cascade stage were doped with Si to 2.6×10^{18} cm^{-3}. Compared to the IC laser near 4.6 μm [32], the number of QWs in the electron injector is reduced from 5 QWs to 4 QWs for the longer lasing wavelength and the doping concentration is also adjusted. The estimated internal loss due to free-carrier absorption is ~6.5 cm^{-1}.

The laser wafer was processed into deep-etched broad-area (150- and 100-μm-wide) mesa stripe lasers and narrow-ridge (nominally 10-, 12-, 15-, and 20-μm-wide) lasers by contact photolithography and wet chemical etching. The processed wafers were typically cleaved into laser bars with a length of 2 mm (unless otherwise specified) and the facets were left uncoated. The laser bars were mounted epilayer side up on copper heat sinks with indium solder, and placed on the cold finger of a cryostat for measurements in cw and pulsed modes. In pulsed measurements, the applied current pulse width was 1 μs at a repetition rate of 5 kHz. When the applied current was larger (e.g. > 6 A), the pulse width was reduced to 150 ns to

avoid possible Joule heating.

In pulsed operation, broad-area (BA) devices made from this IC laser wafer exhibited an emission wavelength near 6 μm at 300 K (Fig. 2) with substantially lower threshold current densities compared to previously reported IC lasers at similar wavelengths. For example, a 150-μm-wide device had a 300K threshold current density J_{th} of 333 A/cm^2 at 6003 nm with a threshold voltage of 4.8 V, corresponding to a threshold input power density of 1.6 kW/cm^2 at 300K, the lowest ever reported among mid-IR semiconductor lasers at similar wavelengths. Compared to a state-of-the-art 7-stage GaSb-based IC laser at 6 μm with the threshold current density of 660 A/cm^2 and threshold voltage of 3.41 V [30, 34], J_{th} of this InAs-based IC laser is reduced by about 50% with a higher voltage efficiency (64.6% vs. 42.4%) and its threshold input power density is also lowered by 29% (1.6 vs. 2.25 kW/cm^2). This BA device lased in cw mode at temperatures up to ~230 K and in pulsed mode at temperatures up to 350 K (limited by the maximum available current) with lasing wavelength red shifted from 5477 nm at 200 K to 6273 nm at 350 K as shown in Fig. 2. As shown in the inset to Fig. 3, another 100-μm-wide device lased at temperatures up to 357 K near 6.28 μm, the highest operating temperature reported for electrically-pumped interband lasers at this wavelength. In Fig. 3, threshold current densities for several representative devices are plotted as a function of the heat-sink temperature, T. The characteristic temperature, T_0 (~38 K in the neighborhood of 300 K), is somewhat lower than that of state-of-the-art GaSb-based IC lasers in the 3-4 μm wavelength region [19].

Narrow-ridge (NR) devices with a top layer of ~4-μm electroplated gold were able to lase in cw mode at higher temperatures than BA devices as indicated in Fig. 3. Due to

isotropic etching with the wet chemical solution, the actual widths of devices were narrower than what were defined by the mask set. For example, the nominal 10-μm-wide ridge device is actually about 7-μm-wide in the cascade region. Their threshold current densities were generally higher than corresponding values for BA lasers as shown in Fig. 3. Also, the threshold current densities of the narrow ridge lasers vary substantially from device to device as shown by two 7-μm-wide narrow-ridge devices in Fig. 3, indicating large non-uniformities in device fabrication with the rough side wall surfaces due to wet etching. For example, at 300 K, the pulsed threshold current density in 7-μm-wide narrow-ridge devices was about 52% to 145% higher than that in a broad-area laser at the same cavity length. The difference is substantially higher than the ~34% difference reported for IC lasers in the 3-4 μm wavelength region [14]. This suggests a somewhat significant current leakage from the sidewalls due to imperfect passivation, which implies further room to achieve better performance by reducing this surface leakage. Nevertheless, a 7-μm-wide narrow-ridge device lased in cw mode at temperatures up to 293 K at 6.01 μm as shown in Fig. 4. The detected output power exceeded 3 mW/facet at 280 K without accounting for beam divergence loss. The Joule heating in the laser was substantial at 293 K, which shows the thermal rollover in Fig.4. The input power at threshold was about 0.66 W at 293 K, which is higher than the state-of-the-art GaSb IC lasers in the 3-4 μm wavelength region [19], but this is still encouraging considering that the lasing was at a significantly longer wavelength. The cw operation of these narrow-ridge IC lasers was affected by their relatively high leakage current and a finite thermal resistance. By comparing threshold current densities in cw and pulsed modes, the specific thermal resistance for the 7-μm-wide ridge lasers was deduced to be in the range 4.4 to 4.6 Kcm^2/kW,

which limited the maximum allowed cw threshold current density below 1 kA/cm^2, as shown in Fig. 3. This suggests there is still room for improving thermal dissipation of these InAs-based IC lasers even without employing epilayer-down mounting.

In summary, InAs-based IC lasers were demonstrated at emission wavelength beyond 6 μm with low threshold current densities and cw operation at room temperature. Further advancements are expected with improvements in thermal management and device fabrication (such as facet coating and dry etching for smooth side walls). There is also room for optimization of device design, considering that there are many adjustable parameters and this is still an early stage of development for this long wavelength spectrum.

Acknowledgments: We thank Wenxiang Huang for calibrating doping concentration. This work was partially supported by the National Science Foundation (IIP-1640576).

REFERENCES

1. R. Q. Yang, “Infrared laser based on intersubband transitions in quantum wells,” at *7th Inter. Conf. on Superlattices, Microstructures and Microdevices*, Banff, Canada, August, 1994; Superlattices and Microstructures, **17** (1), 77-83 (1995).
2. J. Faist, F. Capasso, D. L. Sivco, C. Sirtori, A. L. Hutchinson, and A. Y. Cho, “Quantum Cascade Lasers”, *Science* **264**, 553-556 (1994).
3. R. Q. Yang and J.M. Xu, "Population inversion through resonant interband tunneling", Appl. Phys. Lett. **59**(2), 181-182 (1991).
4. R. Q. Yang and J. M. Xu, "On far-infrared inter-subband lasing in quantum wells", talk at *1991 Inter. Semiconductor Device Research Symp.*, Charlottesville, VA, Dec. 4-6, 1991; pp. 189-192, in its Proc.

5. R. Q. Yang and J.M. Xu, "Leaky quantum wells: A basic theory and applications", Can. J. Phys. **70**(10-11), 1153 (1992).
6. R. Q. Yang, “Phase time delay for interband tunneling in leaky quantum wells”, Phys. Lett. A, **186** (4), 339-344 (1994).
7. R. Q. Yang and J.M. Xu, “Analysis of transmission in polytype interband tunneling heterostructures”, J. Appl. Phys. **72** (10): 4714-4726 (1992).
8. R. Q. Yang, “Type-II interband cascade lasers: From concept to devices”, at 27th International Conference on the Physics of Semiconductors, Flagstaff AZ, July 26-30. 2004; AIP Conf. Proc. **772**, 1553-1554 (2005).
9. Rui Q. Yang, *“*20 years of interband cascade lasers and related devices”, abstract and talk at 12th International Conference on Mid-Infrared Optoelectronics Materials and Devices, Montpellier, France, October 5-9, 2014**.**
10. R. Q. Yang, “Invention of Interband Cascade Lasers – My Journey and Physics” (带间级联激光器的发明—我的经历与物理), 《物理》(Physics) **45 (**1), 46-51 (2016).
11. J. R. Meyer, I. Vurgaftman, R. Q. Yang, and L. R. Ram-Mohan, “Type-II and type-I interband cascade lasers”, Electronics Letters, **32**, 45 (1996).
12. R. Q. Yang, and S. S. Pei, "Novel type-II quantum cascade lasers", J. Appl. Phys. **79**, 8197 (1996).
13. R. Q. Yang, C. J. Hill, K. Mansour, Y. Qiu, A. Soibel, R. Muller and P. Echternach, “Distributed feedback mid-infrared interband cascade lasers at thermoelectric cooler temperatures”, IEEE J. Selected Topics of Quantum Electronics, **13** (5), 1074-1078 (2007).

14. W. W. Bewley, C. L. Canedy, C. S. Kim, M. Kim, J. R. Lindle, J. Abell, I. Vurgaftman, and J. R. Meyer, “Ridge-width dependence of midinfrared interband cascade laser characteristics”, Opt. Eng., **49**, article 111116 (2010).

15. I. Vurgaftman, W. W. Bewley, C. L. Canedy, C. S. Kim, M. Kim, C. D. Merritt, J. Abell, J. R. Lindle, and J. R. Meyer, “Rebalancing of internally generated carriers for mid-infrared interband cascade lasers with very low power consumption”, Nature Communications, **2**, 585 (2011).

16. R. Q. Yang, “Interband Cascade (IC) Lasers”, Chap. 12, in *Semiconductor lasers: fundamentals and applications*, edited by A. Baranov and E. Tournie (Woodhead Publishing Limited, Cambridge, UK, 2013); and 杨瑞青，李路，江宇超，“带间级联激光器:从原始概念到实际器件”，物理学进展， 34(4), 169-190 (2014).

17. R. Weih, M. Kamp, and S. Hofling, "Interband cascade lasers with room temperature threshold current densities below 100 A/cm^2", Appl. Phys. Lett., **102**, 231123 (2013).

18. C. L. Canedy, J. Abell, C. D. Merritt, W. W. Bewley, C. S. Kim, M. Kim, I. Vurgaftman, and J. R. Meyer, "Pulsed and CW performance of 7-stage interband cascade lasers", Opt. Express, **22**, 7702 (2014).

19. I. Vurgaftman, R. Weih, M. Kamp, J R Meyer, C. L. Canedy, C. S. Kim, M. Kim, W. W. Bewley, C. D. Merritt, J. Abell and S. Höfling, “Interband cascade lasers”, J. Phys. D: Appl. Phys. **48** 123001 (2015).

20. C. R. Webster, P. R. Mahaffy, S. K. Atreya, G. J. Flesch, M. A. Mischna, P.-Y. Meslin, K. A. Farley, P. G. Conrad, L. E. Christensen, A. A. Pavlov, *et al.*, “Mars methane detection and variability at Gale crater”, Science **347**, 415 (2015).

21. L. Shterengas, G. Kipshidze, T. Hosoda, *et al*. "Cascade Pumping of 1.9-3.3 μm Type-I Quantum Well GaSb-based Diode Lasers", IEEE Journal of Selected Topics in Quantum Electronics, **23** (6), 1500708 (2017); and references therein.

22. K. Ohtani, and H. Ohno, "An InAs-Based Intersubband Quantum Cascade Laser", Jpn. J. Appl. Phys. **41**, L1279 (2002).

23. R. Teissier, D. Barate, A. Vicet, C. Alibert, A. N. Baranov, X. Marcadet, C. Renard, M. Garcia, C. Sirtori, D. Revin, and J. Cockburn, "Room temperature operation of InAs/AlSb quantum cascade lasers", Appl. Phys. Lett. **85**, 167 (2004).

24. Z. Tian, R. Q. Yang, T. D. Mishima, M. B. Santos, R. T. Hinkey, M. E. Curtis, and M. B. Johnson, "InAs-based interband cascade lasers near 6 μm", Electron. Lett. **45**, 48 (2009).

25. R. Q. Yang, L. Li, L. Zhao, Y. Jiang, Z. Tian, H. Ye, R. T. Hinkey, C. Niu, T. D. Mishima, M. B. Santos, J. C. Keay, M. B. Johnson, and K. Mansour. "Recent progress in development of InAs-based Interband Cascade Lasers" Proc. SPIE **8640**, paper 86400Q (2013).

26. L. Li, H. Ye, Y. Jiang, R. Q. Yang, J. C. Keay, T. D. Mishima, M. B. Santos, M. B. Johnson, "MBE-grown long-wavelength interband cascade lasers on InAs substrates", J. Crystal Growth, **425**, 369-372 (2015).

27. M. Dallner, S. Höfling, M. Kamp, "Room-temperature operation of InAs-based interband-cascade-lasers beyond 6 μm**",** Electron. Lett., **49**, 286 (2013).

28. M Dallner, F Hau, S Höfling, M Kamp, "InAs-based interband-cascade-lasers emitting around 7 μm with threshold current densities below 1 kA/cm^2 at room temperature", Appl. Phys. Lett., **106**, 041108 (2015).

29. R. Q. Yang , L. Li , H. Lotfi, L. Lei, H. Ye , Y. Jiang , SM S. Rassel, J. A. Massengale, T. D. Mishima, M. B. Santos, M. B. Johnson, “Recent Progress in Interband Cascade Devices”, Abstract book of The Forth international workshop on opportunities and challenges in mid-infrared laser-based gas sensing (MIRSENS 4), p31, Wroclaw, Poland, May 15-17, 2017.
30. C. L. Canedy, M. V. Warren, C. D. Merritt, W. W. Bewley, C. S. Kim, M. Kim, I. Vurgaftman, and J. R. Meyer, “Interband cascade lasers with loinger wavelengths”, Proc. SPIE, **10111**, 101110G (2017).
31. A. Schade, and S. Höfling, “Long wavelength Interband Cascade Lasers on GaSb Substrates”, Proc. SPIE, **10403**, 1040305 (2017).
32. L. Li, Y. Jiang, H. Ye, R. Q. Yang, T. D. Mishima, M.B. Santos, and M. B. Johnson, “Low-threshold InAs-based interband cascade lasers operating at high temperatures,” Appl. Phys. Lett, **106** (25), 251102 (2015).
33. R. Q. Yang and J. M. Xu, "Bound and quasibound states in leaky quantum wells", Phys. Rev. B, **46** (11), 6969-6974 (1992).
34. J. R. Meyer, private communications on unpublished data of Naval Research Laboratory (2017).

Figure Captions

Figure 1. Calculated band-edge diagram of one cascade stage and the layer sequence.

Figure 2. Near threshold pulsed lasing spectra of a 150-μm-wide device at various temperatures, where operating current and voltage are provided near corresponding lasing spectral curves.

Figure 3. Threshold current density, J_{th} vs. heat-sink temperature, T, for both broad-area (BA) and narrow-ridge (NR) lasers. The inset is the pulsed lasing spectrum for a 100-μm-wide device at 357 K.

Figure 4. Current-voltage-light characteristics for a 7-μm-wide, 2-mm-long device in cw operation. The inset is the cw lasing spectrum at 293 K.

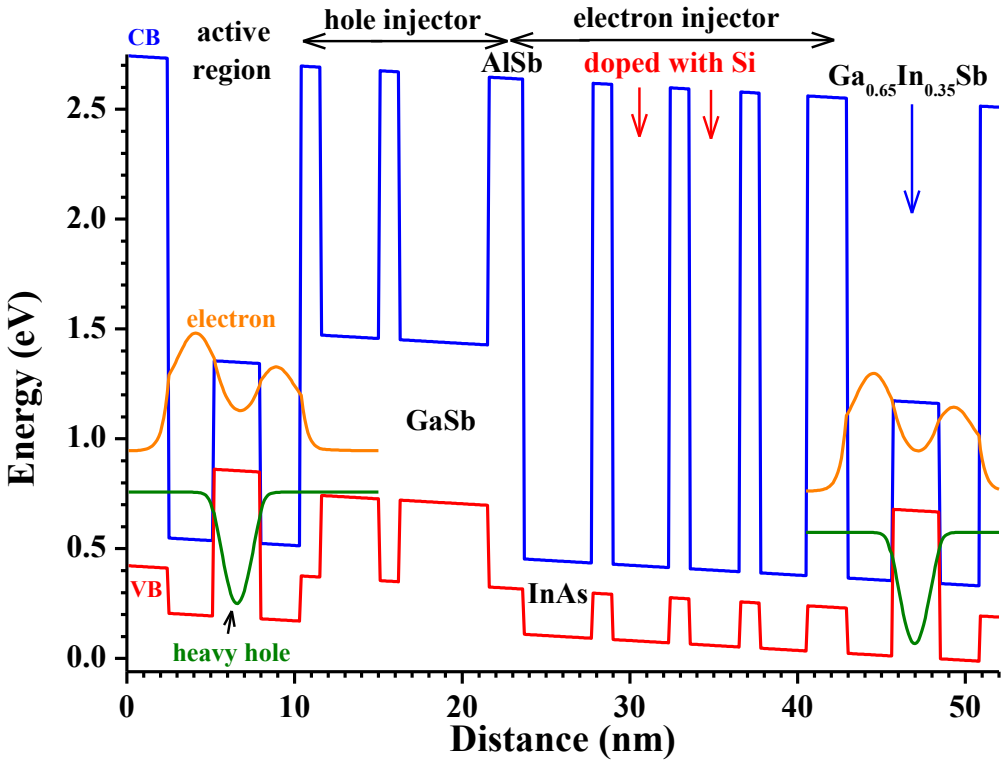

Figure 1. Calculated band-edge diagram of one cascade stage and the layer sequence.

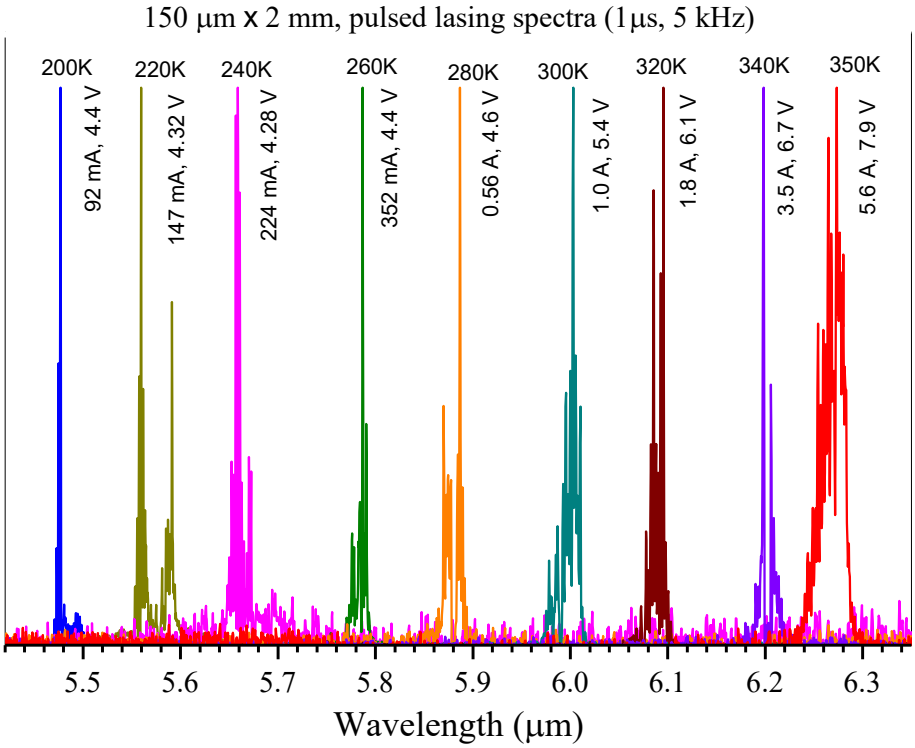

Figure 2. Near threshold pulsed lasing spectra of a 150-µm-wide device at various temperatures.

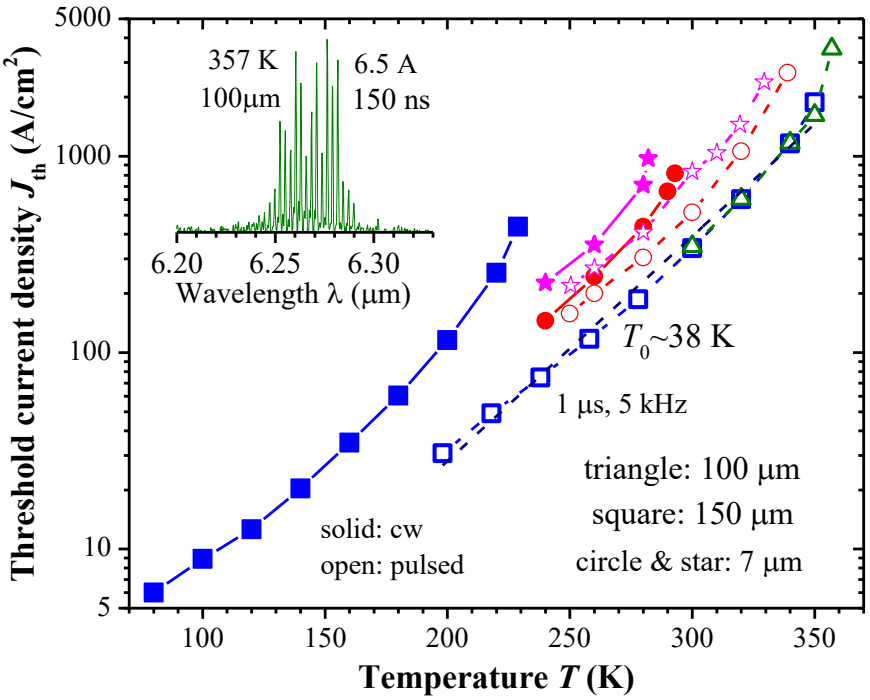

Figure 3. Threshold current density, J_{th} vs. heat-sink temperature, T, for both broad-area (BA) and narrow-ridge (NR) lasers. The inset is the pulsed lasing spectrum for a 100-μm-wide device at 357 K.

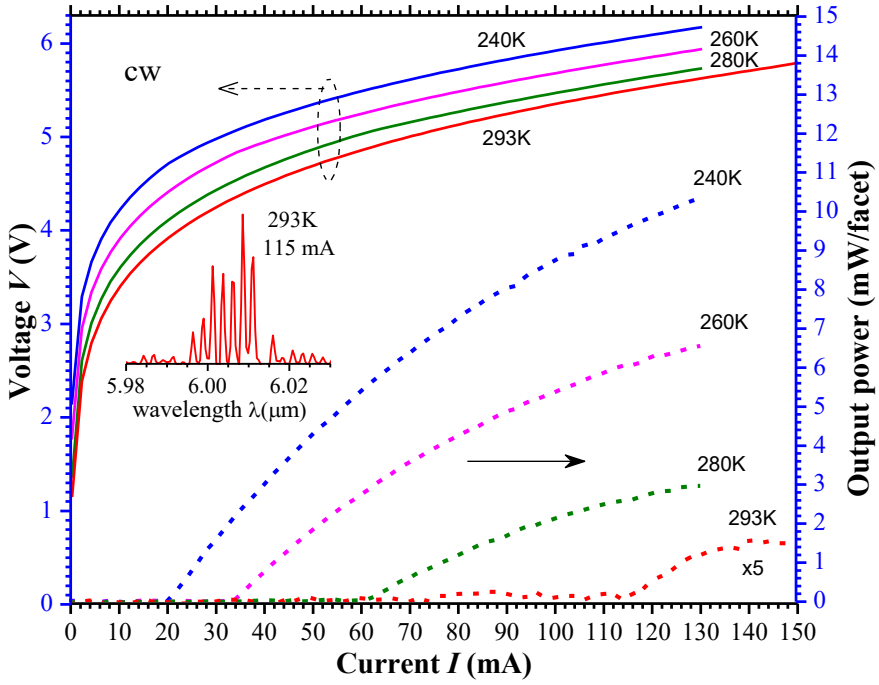

Figure 4. Current-voltage-light characteristics for a 7-μm-wide, 2-mm-long device in cw operation. The inset is the cw lasing spectrum at 293 K.